This is a peer-reviewed, accepted author manuscript of the following research paper: Nobrega, R., Raddo, T., Duarte, U., Glesk, I., Sanches, A., & Loiola, M. L. (2020). Performance analysis of a nanocolumn-RTD VCO for emerging THz wireless applications. In 2020 IEEE Latin-American Conference on Communications (LATINCOM) IEEE. https://doi.org/10.1109/LATINCOM50620.2020.9282323

Performance Analysis of a Nanocolumn-RTD VCO for Emerging THz Wireless Applications

Rafael Nobrega[1,2]
Academic Area of Electrical Engineering
[1]*Federal Institute of Minas Gerais*
Formiga, Brazil
rafael.nobrega@ifmg.edu.br

Thiago Raddo[2]
CECS–Information Engineering
[2]*Federal University of ABC*
Santo Andre, Brazil
thiago.raddo@ufabc.edu.br

Ulysses Duarte[1]
Academic Area of Electrical Engineering
[1]*Federal Institute of Minas Gerais*
Formiga, Brazil
ulysses.rondina@ifmg.edu.br

Ivan Glesk[3]
Faculty of Engineering
[3]*University of Strathclyde*
Glasgow, United Kingdom
ivan.glesk@strath.ac.uk

Anderson Sanches[2]
CECS–Information Engineering
[2]*Federal University of ABC*
Santo Andre, Brazil
anderson.sanches@ufabc.edu.br

Murilo Loiola[2]
CECS–Information Engineering
[2]*Federal University of ABC*
Santo Andre, Brazil
murilo.loiola@ufabc.edu.br

***Abstract*—The data rates which can be processed by integrated communication systems are increasing as the CMOS process and photonic technologies scale. Emerging bandwidth-hungry applications demand new solutions based on terahertz (THz) systems. This work proposes a GaAs/AlAs nanocolumn-Resonant Tunneling Diode (Nano-RTD) device as a voltage-controlled oscillator (VCO) for frequency generation in the THz spectrum window, i.e., Y-band (325 – 500 GHz). A comprehensive semi-analytical approach to evaluating the performance of the Nano-RTD VCO device is developed. The latter addresses the oscillation frequency, maximum oscillation frequency, tuning range, output power, DC consumption power, and DC/AC conversion efficiency. Moreover, the oscillation stability of the designed device in the Y-band was numerically verified. Results shown that the device can operate in the Y-band (@ ∼500 GHz and 300 K), with a very-low DC power consumption down to 0.16 mW, along with a good DC/AC conversion efficiency (2.4%). The Nano-RTD VCO is compatible with current CMOS fabrication technology and has a very compact footprint (2000 nm^2). Finally, the device may be used as part of system solutions to satisfying emerging THz wireless applications such as in-body nano-communication, wireless nano-networks, and network-on-chip.**

***Index Terms*—nanocolumn, resonant tunneling diode, voltage-controlled oscillator, THz applications**

I. Introduction

Quasi-one-dimensional (q-1D) devices based on semiconductor heterostructures have started receiving a great deal of attention due to its potential applications in the terahertz (THz) band (0.1 – 10 THz) [1]. The THz window has a large bandwidth availability and is regarded as part of the solution of next-generation wireless systems and networks. Furthermore, THz-based systems will most likely benefit from high-speed modulation, ultra-low latency, and compact footprint devices [2]. These benefits can be applied to a myriad of applications such as in-body nano-communication, wireless nano-networks, and network-on-chip [3]. Then, new semiconductor heterostructure devices capable of operating at the THz region are becoming of paramount importance for next-generation wireless systems [2], [3]. Nowadays, novel fabrication techniques have contributed significantly to increase the nanotechnology maturity of devices enabling advanced electronic and photonic applications [1]. For instance, it became feasible to assemble nanowires or nanocolumns with embedded semiconductor heterostructures (III-V or Si) [4] to conceive quasi-one-dimensional resonant tunneling diodes (RTD) [5], [6].

Tsu and Esaki envisioned that the RTD [7] and its non-linear current-voltage (*I–V*) curves has resulted in a peculiar feature known as negative differential resistance (NDR). This characteristic helped made the RTD a suitable device for designing oscillating circuits since the NDR effect compensates for the ohmic loss of the resistive elements. Hence, several efforts have been dedicated to producing RTD devices capable of oscillating in high frequencies. Most of the approaches present in the literature present devices operating in the microwave range with frequencies of the order of hundreds of GHz. It has been recently demonstrated that RTDs can reach frequencies up to 2 THz operating at room temperature (300 K) [8]. Nonetheless, such devices have the disadvantage of requiring large footprints to perform accurately. The miniaturization of devices to levels that meet the quasi-one-dimensional nanoelectronics requirements, which include significant RTD downscaling, was first presented with a 40 nm diameter InP/InAs nanowire-RTD (NW-RTD) structure operating at a temperature of 4.2 K in [5]. Afterward, J. Wensorra et al. [6] proposed a similar device with a double-barrier quantum-well (DBQW) formed by GaAs/AlAs with a 50 nm diameter operating at room temperature named nanocolumn-RTD (Nano-RTD).

In this work, we propose and investigate a GaAs/AlAs Nano-RTD VCO for frequency generation in the THz spectrum region commonly named Y-band (325 – 500 GHz). The device operates at room temperature, has a nano footprint and is fabrication compatible with the current CMOS process. Moreover, we derive new semi-analytical mathematical tools

to investigate, characterize, and assess the performance of the designed Nano-RTD VCO device. In order to do so, we extract features of the Nano-RTD VCO NDR, such as current-voltage (*I–V*) and conductance-voltage (*G–V*) to be used in the performance investigation. Accordingly, we investigate the oscillation frequency, maximum oscillation frequency, tuning range, output power, DC consumption power, and DC/AC conversion efficiency. Results indicated that the designed Nano-RTD VCO device can surprisingly operate with ultra-low power consumption down to 0.16 mW and an excellent DC/AC conversion efficiency of 2.4% for oscillation frequencies around 500 GHz. The investigation confirms that the GaAs/AlAs Nano-RTD VCO device can be seen as a prospective candidate to be implemented in chip-scale THz technology, covering a broad range of functions such as feeder structure for nanoantennas, nanosensors, nanodetectors in THz wireless applications like in-body nano-communication, wireless nano-networks, and network-on-chip [2], [3], [9].

This paper is organized as follows: in Section II, we present the structure of the Nano-RTD device used to design the VCO. Next, in Section III, we show the mathematical formalism and the methodology used to investigate the device. Section IV, we present the results and the performance analysis of the Nano-RTD VCO. Finally, Section V addresses remarkably conclusions.

II. Nano-RTD Device Structure

The VCO device designed and addressed in this work is based on the Nano-RTD manufactured in [6]. The two-terminal device is made in a 50 nm diameter GaAs nanocolumn with two built-in barriers (thickness 1.7 nm) separated by a 5 nm GaAs layer forming the quantum-well. The schematic representation of the manufactured Nano-RTD can be seen in Fig. 1-(a), while the other semiconductor layers are grown epitaxially, containing the thickness and doping information for each layer, are shown in Fig. 1-(b). According to the experimental results, the peak-to-valley current ratio (PVCR) of the 50 nm diameter device is equivalent to the 300 nm diameter device [6]. The PVCR between 50 and 300 nm decreases at most 40%, from 2.1 to 1.25. This behavior is due to the quantum collimation effect [6], i.e., there is a narrowing of the channel produced by the depletion regions of the lateral surfaces of the cylindrical nanocolumn, decreasing the radius of 25 nm to a smaller value R', as shown in Fig. 1-(a). Such peculiarity allows the downscaling of the device, maintaining the similar performance of Nano-RTDs with a diameter greater than 300 nm [6].

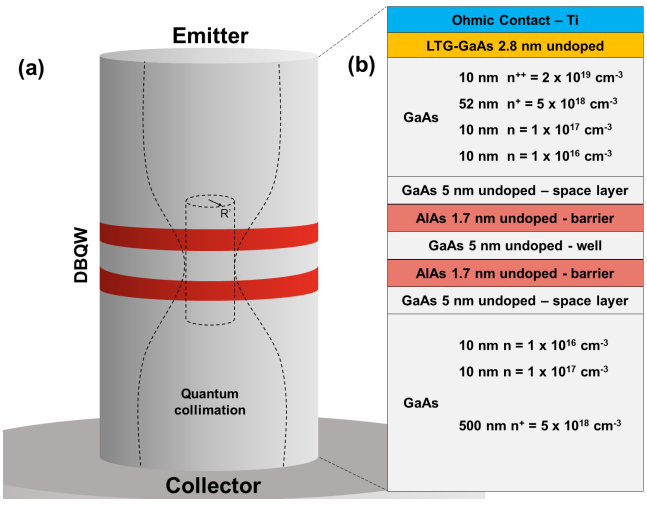

Fig. 1. Schematic representation of: (a) 50-nm GaAs/AlAs nanocolumn-resonant tunneling diode (Nano-RTD). (b) cross-sectional view of the device with the double-barrier quantum-well (DBQW) structure inside the Nano-RTD. Figure adapted from [6].

III. Mathematical Framework and Methodology

This section presents the proposed semi-analytical formalism and the methodology for the design of the 50 nm GaAs/AlAs Nano-RTD VCO. First, it is necessary to extract the experimental Nano-RTD curve characterized by J. Wensorra et al. [6]. Several works address fitting functions to extract and reproduce the conventional RTD *I–V* curves [10]–[12]. Here, we propose a new *I–V* curve fitting function for these q-1D devices with DBQW structure, and it can be expressed as

$$F(V) = \begin{cases} a_1 e^{b_1 V} + c_1 e^{d_1 V}, & V \leq V_p \\ -a_2 \sin V + b_2 (V - d_2)^2 + c_2, & V > V_p \end{cases} \quad (1)$$

where a_1, b_1, c_1, d_1, a_2, b_2, c_2 and d_2 are fitting parameters, V_p is the peak voltage of the *I–V* curve. *G–V* expression is obtained by differentiating $F(V)$ with respect to voltage

$$G(V) = \begin{cases} a_1 b_1 e^{b_1 V} + c_1 d_1 e^{d_1 V}, & V \leq V_p \\ -a_2 \cos V + 2 b_2 (V - d_2), & V > V_p \end{cases} \quad (2)$$

the values of the fitting parameters were a_1 = 9.112 $\times$ 10^{-10}, b_1 = 4.917, c_1 = -1.044 $\times$ 10^{-9}, d_1 = 4.769, a_2 = 1.916 $\times$ 10^{-6}, b_2 = 2.555 $\times$ 10^{-8}, c_2 = 2.076 $\times$ 10^{-7}, and d_2 = 10. They were optimized based on the experimental data, resulting in an adjusted R-square of 99.6%. The comparisons of the *I–V* and *G–V* curves of Eqs. (1) and (2), respectively, with the experimental data are shown in Fig. 2. The primary information of the NDR region is the peak current (I_p) and voltage (V_p), valley current (I_v) and voltage (V_v), and PVCR, whose values were obtained by fitting: I_p = 133.5 nA, I_v = 59.62 nA, V_p = 1.516 V, V_v = 1.792 V, and PVCR = 2.2.

The equivalent electrical circuit of the Nano-RTD VCO is depicted in Fig. 3. Considering the large-signal analysis, the Nano-RTD is connected to a DC power supply (V_{in}), via a resistor (R_s) and an inductor (L_s) in series. Furthermore, the Nano-RTD can be represented by the current source $F(V)$, Eq. (1), in parallel with the capacitance of the device C_D. In this situation, the device's inductance (L_{qw}) is neglected due to its small value in relation to L_s ($L_{qw} \ll L_s$) [13]. C_D is given by

$$C_D(V) = -\tau_{RTD} G_D(V) + \frac{Area}{\frac{L_w}{\varepsilon_w} + \frac{2L_b}{\varepsilon_b} + \frac{L_{dep}(V)}{\varepsilon_{dep}}}, \quad (3)$$

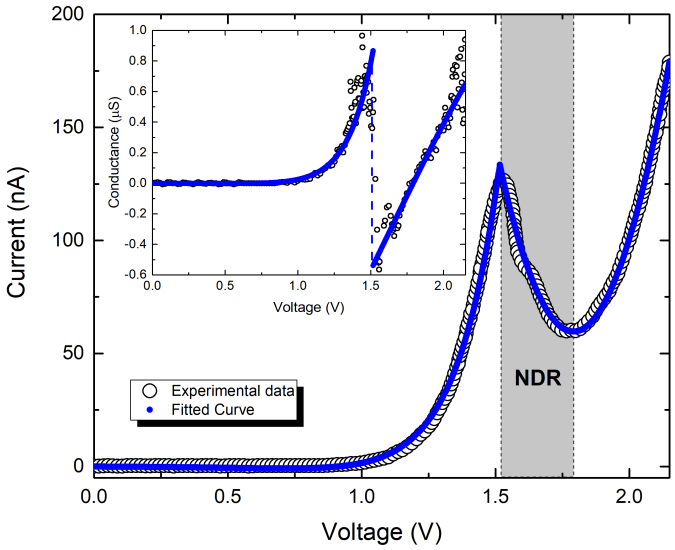

Fig. 2. Comparison of the analytical and experimental *I–V* curves. Inset: comparison of the analytical and experimental *G–V* curves. Experimental data extracted from [6].

where τ_{RTD} is the carrier transit time, G_D is the conductance described by Eq. (2), L_w is the length of the quantum-well, L_b is the length of the barriers, ε_w, ε_b, and ε_{dep} are the dieletric permittivities of the quantum-well, barriers and depletion region. The width of the depletion region is calculated using the analytical expression presented in our previous work [14]

$$L_{dep}(V) = \left[\frac{2\varepsilon_{dep}V_{in}}{q}\left(\frac{1}{N_a}+\frac{1}{N_d}\right)\right]^{M}, \tag{4}$$

where q is the electronic charge, N_a and N_d are the densities of acceptors and donors, respectively, and M = 0.6673 (fitting factor), the validation of Eq. (4) was developed in [14].

Now, τ_{RTD} is expressed as [13]

$$\tau_{RTD} = \frac{\hbar}{E_1}e^{2L_b\frac{\sqrt{2m_b(U_0-E_1)}}{\hbar}}, \tag{5}$$

where $\hbar$ is the reduced Planck constant, m_b is the effective mass of the barrier, U_0 is the height of the barrier, and E_1 is the first energy level of the DBQW structure. Figure 1-(a) illustrates the effect of quantum collimation on the device channel, this narrowing can be approximated to a reduce cylindrical nanowire, with a radius R' smaller than the radius R of the manufactured nanocolumn ($R' < R$). In this way, to calculate E_1, we use the numerical method known as Transfer-Matrix Method (TMM) developed by Tsu and Esaki [7], and extended to cylindrical symmetry in [15]. Thereby, we simulate the transmission coefficient of the Nano-RTD and determine the value of E_1 = 0.108 eV, considering R' = 6 nm. Comparing this value of E_1 with the value of E_1 = 0.11 eV available in [6], we have a 98.2% agreement, i.e., the quantum collimation effect resulted in R' four times less than R, approximately.

The numerical values of the parameters used to determine τ_{RTD} Eq. (5), L_{dep} Eq. (4), and C_D Eq.(3) are: U_0 = 0.5 eV, E_1 = 0.108 eV, $m_b = 0.13m_0$, $m_w = 0.067m_0$, L_b = 1.7 nm, L_w = 5 nm, N_a = 1.2 × 10^{15} cm^{-3}, N_d = 2 × 10^{19} cm^{-3}, $V_{in} \in$ [1.516 V, 1.792 V], $\varepsilon_w = \varepsilon_{dep} = 13.1\varepsilon_0$, $\varepsilon_b = 10.1\varepsilon_0$, and $Area$ = 2 × 10^{-15} m^2.

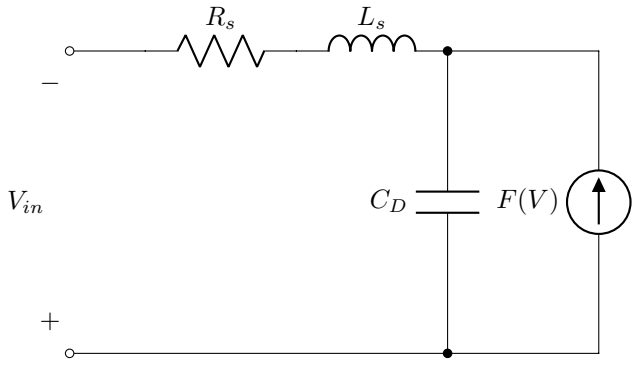

Fig. 3. Equivalent circuit of the Nano-RTD VCO (large-signal analysis) [13].

Using Eq. (5), we obtain the value of τ_{RTD} equal to 186 fs. To check the validity of the obtained τ_{RTD}, we use the following expression [16]

$$\tau_{RTD} = \tau_{dwell} + \frac{\tau_{dep}}{2}, \tag{6}$$

where τ_{dwell} is the transit time through the DBQW structure, and τ_{dep} is the transit time through the collector depletion region. The Nano-RTD has an electric field value of 1.6 × 10^3 kV/m, and then, it is possible to obtain the value of the carrier saturation velocity in GaAs, v_s = 1.2 × 10^7 cm/s [17]. With the values of the width of the DBQW structure, 13.4 nm, and the width of the depletion region, 15.5 nm (average value), we can estimate τ_{dwell} and τ_{dep} equal to 111 fs and 130 fs, respectively. Substituting these values in Eq. (6), we calculate τ_{RTD} = 176 fs. Comparing 186 fs, and 176 fs, we find an agreement around 95%, validating the use of Eq. (5). From Eq. (3), we calculate average C_D in NDR equal to 9.1 aF, using the formula proposed by J. Jo et al. [18], we obtain the average C_D equal to 8.8 aF, resulting in a agreement around 97%. Furthermore, with τ_{RTD} given by Eq. (5) it is possible to calculate the intrinsic high frequency limit of the Nano-RTD as follows [19]

$$f_{int-limit} = \frac{1}{4\tau_{RTD}}. \tag{7}$$

From the total impedance of the device, we can obtain expressions that describe the oscillation frequency (f_{osc}) and the maximum frequency (f_{max}) of the Nano-RTD VCO as [13]

$$f_{osc} = \frac{1}{2\pi}\sqrt{\frac{1}{L_sC_D} - \left(\frac{G_D}{C_D}\right)^2}, \tag{8}$$

$$f_{max} = \frac{1}{2\pi C_D}\sqrt{-\frac{G_D}{R_s} - G_D^2}, \tag{9}$$

respectively, where L_s and R_s will directly affect the performance of the Nano-RTD VCO, so it is up to the designer to

define them to operate in a given f_{osc}. Emphasizing that, f_{osc} and f_{max} are limited by the device's $f_{int-limit}$.

The oscillation stability condition of the Nano-RTD based VCO, as a function of R_s and L_s, was verified by numerically solving the following system of differential equations

$$\begin{cases} \frac{dV(t)}{dt} = \frac{1}{C_D}\left(I\left(t\right) - F(V)\right) \\ \frac{dI(t)}{dt} = \frac{1}{L_s}\left(V_{in} - RI(t) - V(t)\right) \end{cases} \tag{10}$$

using the Runge–Kutta Method–ode45 (MATLAB). Satisfying the stability criterion, $V(t)$ and $I(t)$ will be the voltage and current sine waves, respectively, at the output of the device, as shown in Fig. 4-(a). In Fig. 4-(b), we visualize a stable orbit in the current-voltage phase space, i.e., $V(t)$ and $I(t)$ represent harmonic oscillations without damping.

The maximum output power of the device is obtained using the following equation

$$P_{max} = \frac{3}{16}\Delta I \Delta V, \tag{11}$$

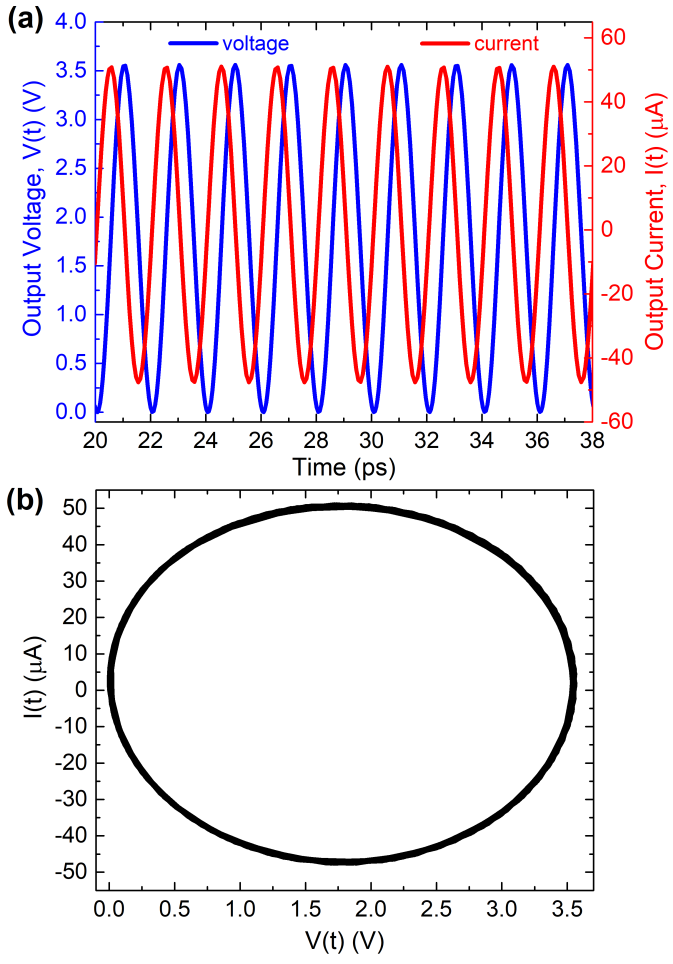

Fig. 4. (a) Output voltage and current as a function of time obtained numerically. (b) Current-voltage phase space of the Nano-RTD VCO, indicating a stable orbit for V_{in} = 1.78 V.

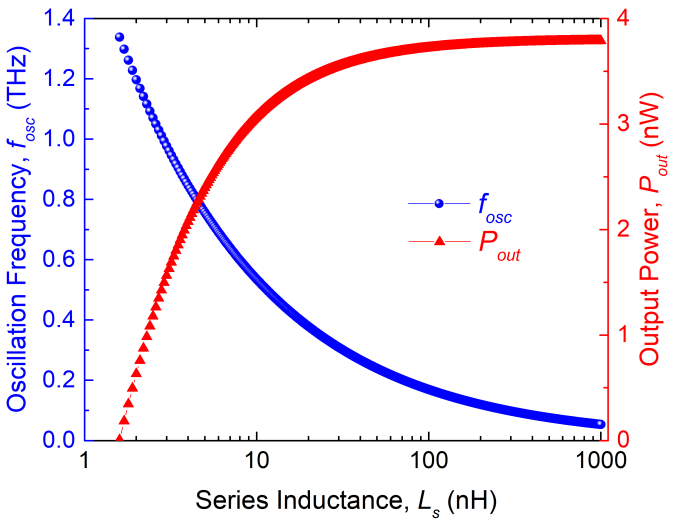

Fig. 5. Oscillation frequency and output power of Nano-RTD VCO as a function of series inductance for C_D = 8.84 aF and V_{in} = 1.78 V.

where $\Delta I = I_p - I_v$, and $\Delta V = V_v - V_p$ [13]. However, the P_{max} is degraded by the high operating frequency and will be expressed as [19]

$$P_{out} = \frac{3}{16}\Delta I \Delta V \cos\left(\omega \tau_{RTD}\right), \tag{12}$$

the DC consumption power of the system is given by [13]

$$P_{DC} = \left(I_p - \frac{\Delta I}{2}\right)\left(V_p + \frac{\Delta V}{2}\right), \tag{13}$$

and finally, the DC/AC conversion efficiency can be calculated as [13]

$$\eta = \frac{P_{max}}{P_{DC}}. \tag{14}$$

Thus, in this section, we present how to calculate the main parameters of the Nano-RTD VCO and the figures of merit that will be used to evaluate its performance.

IV. Results and Discussion

Based on the methodology described above, we developed the performance analysis of the Nano-RTD VCO operating in the Y-band (325 – 500 GHz) [22]. The VCO was designed to work at frequencies of up to 500 GHz. To meet this requirement, L_s must be 12 nH, as shown in Fig. 5. Noting that, following Eq. (7), the proposed system has an $f_{int-limit}$ of 1.34 THz. For each V_{in} in the device NDR, we will have a distinct and stable solution set of $V(t)$, $I(t)$, f_{osc}, f_{max}, and P_{out}, whose values are shown in Table I. The f_{osc}^{anal} validation (Eq. 8) was verified by comparing it with the f_{osc}^{num} (Eq. (10)), considering that the errors were around 1%, according to values presented in Table I. Then, we have a Nano-RTD VCO operating range of 480.2 to 498.7 GHz, which represents a tuning range (TR) of 4%, for supply voltage (SV) from 1.52 to 1.78 V. Furthermore, the f_{max} was obtained at around 844 GHz for V_{in} = 1.78 V, and the P_{out} was around 3.2 nW (-55

TABLE I
PERFORMANCE ANALYSIS OF THE NANO-RTD VCO DESIGNED TO OPERATE IN THE Y-BAND

V_{in} (V)	R_s (Ω)	f_{osc}^{num*} (GHz)	f_{osc}^{anal} (GHz)	f_{max} (GHz)	P_{out} (nW)
1.52	615	473.8	480.2	493.3	3.21
1.54	583	475	481.6	506.6	3.2
1.56	550	476.2	483.1	521.6	3.2
1.58	516	477.5	484.5	538.6	3.2
1.60	485	478.9	486	555.5	3.19
1.62	453	480.4	487.4	574.8	3.19
1.64	421	481.8	488.9	596.2	3.19
1.66	390	483.3	490.3	619.5	3.18
1.68	359	484.8	491.7	645.7	3.18
1.70	328	486.3	493.1	675.1	3.18
1.72	298	487.7	494.5	708.7	3.17
1.74	268	489.2	495.9	747.3	3.17
1.76	238	490.6	497.3	792.2	3.17
1.78	210	492.1	498.7	843.5	3.16

(*) Error between f_{osc}^{num} and f_{osc}^{anal} around 1%

dBm). Using Eq. (13) and (14), we calculate the P_{DC} and η to 0.16 mW and 2.4%, respectively.

The Nano-RTD is a device that has peculiar features since it has reduced dimensions (50 nm diameter), and even so, it presents the NDR region at room temperature (300 K). Other similar devices, generally, are nanowire-RTDs, operating at a cryogenic temperature [5], or when operating at room temperature, it presents a reduced NDR region and a PVCR around 1.2 [20]. In this context, it was difficult to find another experimental characterized q-1D devices in the technical literature working as VCO in THz oscillation frequencies (∼0.5 THz), at room temperature. Thus, we compare the performance of the Nano-RTD VCO proposed here (manufactured by J. Wensorra et al. [6]) with VCOs of different technologies operating in Y-band and 300 K [21]–[24]. The values of the main parameters of the VCOs are shown in Table II. The Nano-RTD VCO showed a tuning range (TR) around 4%, which is considered a small value about the other bulk RTDs (56%). Such discrepancy is due to the different characteristics of the NDR of each device. The nanodevice presents a great inclination of the NDR, $G_D \sim \Delta I/\Delta V$, which limits its TR. To improve its TR, the nanodevice should have been manufactured with an optimized relationship between the length of barriers (L_b) and the quantum-well (L_w) in DBQW, so that the value of ΔV is increased, thus implying an increase in TR. Analyzing Table II, we found that the DC consumption power (P_{DC}) of the Nano-RTD VCO is the lowest compared to the other devices. This reduced value of the nanodevice is due to its miniaturization that resulted in a peak current around 130 nA. The P_{DC} is represented by Eq. (13), and like the TR, its value could be improved, as long as L_b and L_w are chosen, in order to result in optimized ΔI and ΔV values. This study relating L_b and L_w to ΔI and ΔV of the nanodevice will be developed later. Emphasizing that, this low PDC value means low energy consumption, which combined with the efficiency of 2.4%, the highest among the other devices presented in Table II, makes the Nano-RTD VCO a potential candidate for

TABLE II
COMPARISON WITH STATE-OF-THE-ART VCOS IN THE Y-BAND

Parameters	**This work**	[21]	[22]	[23]	[24]
Technology	Nano RTD	Bulk RTD†	28 nm†	40 nm†	45 nm†
f_{osc} (GHz)	480-499	327-580	409-414	475-511	410
TR (%)	4	56	1.2	7.5	NT
P_{out} (dBm)	-55	-46.2	-17.3	-15.3	-47
P_{DC} (mW)	0.16	9.9	120	17.1	16.5
η (%)	2.4	0.24	0.02	0.17	10^{-3}
A (μm^2)	10^{-3}‡	1.2‡	–	10^5	10^5
SV (V)	1.52-1.78	0.41-0.77	1.5	0.55-0.9	1.5

†including antenna ‡ only device area NT = Non-tunable

energy-saving applications.

Table II shows that the Nano-RTD VCO presented the lowest P_{out}. In comparison with the bulk RTD and the 45 nm CMOS, the nanodevice's P_{out} was around 9 dB lower. This reduced P_{out} value of the Nano-RTD VCO is due to the $I_p \sim 130$ nA. An alternative to improve the output power of this VCO would be to connect Nano-RTDs in parallel so that the P_{out} would be increased to the desired design levels. However, the system's oscillation frequency would be reduced. Furthermore, considering the integration of a proper nano-antenna (impedance matching) with the Nano-RTD (as designed for the RTDs-Bulk in the Table II, this VCO can become a potential candidate for applications in THz wireless nano-communication systems.

Finally, in Table II, we find that the nanodevice has the smallest footprint area. Thus, the Nano-RTD VCO has dimensions and requirements to be applied as a nanoantenna feeder structure in wireless nano-communication systems operating in the THz band [2], [3]. The performance analysis of the THz wireless link using the Nano-RTD VCO will be developed later.

V. CONCLUSION

In this paper, the performance of a 50 nm GaAs/AlAs Nano-RTD VCO device was investigated by using a semi-analytical approach. A new mathematical formalism was derived, validated, and used for performance analysis of the designed device. Fitting curves from experimental data were used to extract the current-voltage (*I–V*) and conductance-voltage (*G–V*). The performance of the device was compared against its state-of-the-art counterparts operating in the Y-band (325 – 500 GHz) and at room temperature. The results indicated that the device is capable of operating at THz window with ultra-low levels of power consumption (i.e., 160 μW), and an excellent DC/AC conversion efficiency of 2.4% @ ∼500 GHz. Hence, the Nano-RTD VCO device can be considered as part of a potential solution for systems designed to accommodate emerging THz applications such as in-body nano-communication, wireless nano-networks, and network-on-chip.

REFERENCES

[1] K. Sengupta, T. Nagatsuma, and D. Mittleman, "THz integrated electronic and hybrid electronic-photonic systems," Nature Electronics, vol. 1, pp. 622–635, December 2018.

[2] H. Elayan, O. Amin, B. Shihada, R. Shubair, and Alouini, "Terahertz Band: The Last Piece of RF Spectrum Puzzle for Communication Systems," IEEE Open Journal of the Communications Society, vol. 1, pp. 1–32, January 2020.

[3] F. Lemic, et al., "Survey on Terahertz Nanocommunication and Networking: A Top-Down Perspective," arXiv:1909.05703, September 2019.

[4] S. Benter et al., "Quasi One-Dimensional Metal-Semiconductor Heterostructures," Nano Letters, vol. 19, pp. 3892–3897, May 2019.

[5] M. Björk et al., "Nanowire Resonant Tunneling Diodes," Applied Physics Letters, vol. 81, pp. 4458–4460, November 2002.

[6] J. Wensorra, K. Indlekofer, M. Lepsa, A. Forster, and H. Luth, "Resonant Tunneling in Nanocolumns Improved by Quantum Collimation," Nano Letters, vol. 5, pp. 2470–2475, December 2005.

[7] R. Tsu, and L. Esaki, "Tunneling in a Finite Superlattice," Applied Physics Letters, vol. 22, pp. 562–564, June 1973.

[8] R. Izumi, S. Suzuki and M. Asada, "1.98 THz resonant-tunneling-diode oscillator with reduced conduction loss by thick antenna electrode," 2017 42nd International Conference on Infrared, Millimeter, and Terahertz Waves (IRMMW-THz), Cancun, 2017, pp. 1-2.

[9] A. Galal, and X. Hesselbach, "Nano-networks communication architecture: Modeling and functions," Nano Communication Networks, vol. 17, pp. 45-62, September 2018.

[10] J. N. Schulman, H. J. De Los Santos, and D. H. Chow, "Physics-based RTD current-voltage equation," IEEE Electron Device Letters, vol. 17, pp. 220–222, May 1996.

[11] S. F. Nafea, and A. A. S. Dessouki, "An accurate large-signal SPICE model for Resonant Tunneling Diode," 2010 International Conference on Microelectronics, Cairo, 2010, pp. 507–510.

[12] R. M. Abdallah, A. A. S. Dessouki, and M. H. Aly, " The resonant tunneling diode characterization for high frequency communication system," Microelectronics Journal, vol. 75, pp. 1–14, May 2018.

[13] J. Figueiredo, *Optoelectronic Properties of Resonant Tunneling Diodes*. PhD thesis, Universidade do Porto, 2000.

[14] R. Nobrega, U. Duarte, T. Raddo, I. Glesk, A. Sanches, and M. Loiola, "A Semi-Analytical Approach for Performance Evaluation of RTD-Based Oscillators," 2019 21st International Conference on Transparent Optical Networks (ICTON), Angers, France, 2019, pp. 1-4.

[15] R. Ragi, R. Nobrega, and M. Romero, "Modeling of Peak Voltage and Current of Nanowire Resonant Tunneling Devices: Case Study on InAs/InP Double-Barrier Heterostructures," International Journal of Numerical Modelling: Electronics Networks, Devices and Fields, vol. 26, pp. 506–517, July 2013.

[16] N. Orihashi, S. Hattori, S. Suzuki and M. Asada , "Experimental and Theoretical Characteristics of Sub-Terahertz and Terahertz Oscillations of Resonant Tunneling Diodes Integrated with Slot Antennas," Japanese Journal of Applied Physics, vol. 44, pp. 7809–7815, November 2005.

[17] H. Arabshahi, M. Khalvati, and M. Rokn-Abadi, "Temperature and Doping Dependencies of Electron Mobility in InAs, AlAs and AlGaAs at High Electric Field Application," Brazilian Journal of Physics, vol. 38, pp. 293–296, September 2008.

[18] J. Jo, H. S. Li, Y. Chen, and K. Wang , "Observation of a Large Capacitive Current in a Double Barrier Resonant Tunneling Diode at Resonance," Applied Physics Letters, vol. 64, pp. 2276–2278, April 1994.

[19] S. Muttlak, O. Abdulwahid, J. Sexton, M. Kelly and M. Missous, "InGaAs/AlAs Resonant Tunneling Diodes for THz Applications: An Experimental Investigation," in IEEE Journal of the Electron Devices Society, vol. 6, pp. 254–262, February 2018.

[20] Y. Shao, S. D. Carnevale, A. T. Sarwar, R. C. Myers, and W. Lu, "Single nanowire AlN/GaN double barrier resonant tunneling diodes with bipolar tunneling at room and cryogenic temperatures," Journal of Vacuum Science & Technology B, vol. 31, 06FA03, November 2013.

[21] S. Kitagawa, S. Suzuki, and M. Asada, "Wide-Range Varactor-Tuned Terahertz Oscillator Using Resonant Tunneling Diode," Journal of Infrared, Millimeter, and Terahertz Waves, vol. 35, pp. 445–450, March 2014.

[22] A. Standaert, and P. Reynaert, "A 410 GHz OOK Transmitter in 28 nm CMOS for Short Distance Chip-to-Chip Communications," 2018 IEEE Radio Frequency Integrated Circuits Symposium (RFIC), Philadelphia, PA, 2018, pp. 240–243.

[23] K. Guo, and P. Reynaert, "A 475–511GHz Radiating Source with SIW-Based Harmonic Power Extractor in 40 nm CMOS," 2017 IEEE MTT-S International Microwave Symposium (IMS), Honolulu, HI, 2017, pp. 95–98.

[24] E. Seok et al., "A 410GHz CMOS Push-Push Oscillator with an On-Chip Patch Antenna," 2008 IEEE International Solid-State Circuits Conference - Digest of Technical Papers, San Francisco, CA, 2008, pp. 472–629.